Cite this: DOI: 10.1039/c0xx00000x

www.rsc.org/xxxxxx

ARTICLE TYPE

Cu^{2+} ions Induce the Growth of Porous Co_3O_4 Nanospheres as High Capacity Supercapacitor

Rongmei Liu,*[a] Zixiang Jiang,[a] Qi Liu,[b] Xiandong Zhu[a] and Weiye Chen[a]

Received (in XXX, XXX) Xth XXXXXXXXX 20XX, Accepted Xth XXXXXXXXX 20XX

DOI: 10.1039/b000000x

Abstract: In this study, porous Co_3O_4 nanospheres were controllably synthesized by applying metal ions Cu^{2+} as structure-inducing agent. The growth of the Co_3O_4 nanostructures was induced by metal ions without the addition of any other surfactants. The porous Co_3O_4 nanospheres were composed of nanosheets. When used as electrode material in supercapacitor, the porous Co_3O_4 nanospheres exhibit much better capacitive properties of 246.7 F g^{-1} than commercial Co_3O_4 powder at current density of 0.5 A g^{-1}, maintaining 86 % of the initial capacity at current density of 1 A g^{-1} after 500 cycles. Such high performance can be attributed to the desirable morphology. The results manifest that porous Co_3O_4 nanospheres composed with nanosheets are promising electrode material for supercapacitor.

Introduction

Cobalt oxide, as an important transition metal oxide, has been widely studied and used in many fields such as gas-sensors,[1-4] heterogeneous catalyses,[5,6] lithium-ion batteries,[7,8] supercapacitors[9-11] and magnetic materials[12] due to its conspicuous physical-chemical properties and low-costs. As electrode material for supercapacitors, cobalt oxide was thought to be one of the most promising electrode material for next-generation high-performance supercapacitors for its high theoretical specific capacitance, good electrochemical reversibility, and low costs.[13] Cobalt oxide with nano size has attracted great interests due to the significant nano-effects different from those of bulk materials. Diverse shapes and morphologies of cobalt oxide nanomaterials such as wires,[14] rods,[15] tubes,[16] polyhedrons,[17] sheets,[6] flowers[18] and spheres[19] were successfully synthesized. Among these shapes, nanomaterials with porous or hollow structures have been received much attention because of their high surface area, fast ion transfer and many exposed centers, which show great application potentials in batteries, absorbents, catalysts etc. Up to now, many methods have been used to fabricate Co_3O_4 hollow structures such as complex precursor-calcination method,[20, 21] template-based chemical vapor deposition,[22] solvothermal treatment,[23] and micro-emulsion method[24] and so on. In these methods, complex precursor-calcination method is the most used method. For example, Du *et. al.* first prepared one-dimensional cobalt acetate hydroxide ($Co_5(OH)_2(CH_3COO)_8 \cdot 2H_2O$) prisms precursor, and then through thermal decomposition synthesized hollow Co_3O_4 nanoboxes.[20] Shi *et. al.* obtained one-dimensional Co_3O_4 nanotubes by thermal decomposition of Co(III) complex with strong intermolecular hydrogen bonding precursors.[16]

Metal ions have been demonstrated to control the shape and morphology of the nanomaterials.[25] We have used different metal ions as structure-inducing agents to synthesize different shaped α-Fe_2O_3 nanocrystals.[26] In this paper, we provided a new method to controlled synthesize of porous and hollow Co_3O_4 nanospheres by using metal ions Cu^{2+} as structure-inducing agent and ammonium solution as alkali source through hydrothermal reaction. The porous Co_3O_4 nanospheres were composed of nanosheets. In the electrochemical measurements, the porous Co_3O_4 nanospheres exhibit much better capacitive properties of 246.7 F g^{-1} than commercial Co_3O_4 powder at current density of 0.5 A g^{-1}, maintaining 86 % of the initial capacity at current density of 1 A g^{-1} after 500 cycles. Such high performances can be attributed to the desirable exposed facet and morphology. The results manifest that porous Co_3O_4 nanospheres composed with nanosheets are promising electrode material for supercapacitor.

Experimental Section

Preparation of porous Co_3O_4 nanospheres

In a typical procedure, the starting solution was prepared by mixing 0.199 g of copper acetate (analytically pure) in 10 mL of 0.2 M $CoSO_4$ solution under magnetic stirring. Then 1 mL of ammonia solution (25 %, analytically pure) was added. After 10 min of stirring, the mixture was transferred to and sealed in a 50 mL Teflon-lined autoclave, kept at 160 °C for 12 h, and finally cooled to room temperature. The precipitate was collected by centrifugation (10000 rpm, 1 min), washed alternately with deionized water and ethanol, and dried in air under ambient conditions.

[a] *College of Biological and Chemical Engineering, Anhui Polytechnic University, Wuhu Anhui 241000, P. R. China,*
Fax: +86 553 2871 255; Tel: +86 553 2871 255
E-mail: liurongmei@ahpu.edu.cn
[b] *College of Materials Science and Engineering, Anhui Polytechnic University, Wuhu, Anhui 241000, P. R. China.*

Characterization

Scanning electron microscopy (SEM) characterizations were performed on Hitachi S-4800 at 5 kV. Transmission electron microscopy (TEM) images were obtained using a JEOL JEM-2100 transmission electron microscope operating at 200 kV. Powder X-ray diffraction (XRD) patterns were collected using a Bruker D8 ADVANCE diffractometer with Cu Kα radiation (λ = 1.5418 Å). X-ray photoelectron spectra (XPS) was collected on an ESCALab MKII X-ray photoelectron spectrometer, using nonmonochromatized Al Kα X-ray as excitation source. The binding energies were corrected for specimen charging by calibrating the C1s peak to 284.6 eV.

Electrochemical measurements

In the electrochemical experiments, we used the traditional three electrode system. The working electrode was prepared by mixing 80 wt% of electroactive material (Co_3O_4), 15 wt% of acetylene black, and 5 wt% of polytetrafluoroethylene. This mixture was then pressed onto the foamed nickel electrode and dried at 60 °C for 12 h. The used electrolyte was 1 M KOH aqueous solution. The capacitive performance of the samples was evaluated on a CHI 660e electrochemical workstation. Cyclic voltammetry and chronopotentiometry were tested with a three-electrode cell where Pt wire serves as the counter electrode and a standard calomel electrode (SCE) as the reference electrode.

Results and discussion

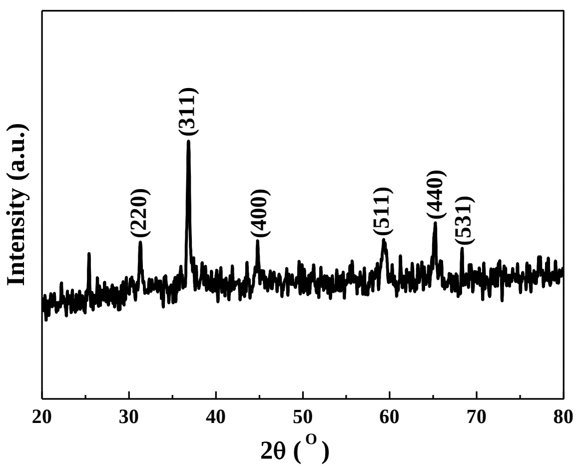

Fig. 1 XRD pattern of the obtained sample.

The porous nanospheres were prepared by hydrothermally treating the mixture of $CoSO_4$ and ammonium solution with metal salt of $CuAc_2$. Fig. 1 presents XRD pattern of the as-prepared sample controlled by Cu^{2+}. Almost all the diffraction peaks can be indexed to the cubic phase of Co_3O_4 (JCPDS 73-1701), indicating that relatively pure Co_3O_4 products were obtained under synthetic conditions. Since the synthesis system has Cu element, XPS measurements were also used to identify the content of Cu. Fig. 2a demonstrates the presence of Co, Cu and O elements. The high resolution XPS spectrum in Fig. 2b shows binding energies of $Cu2p_{3/2}$ and $Cu2p_{1/2}$ corresponding to 933 eV and 953 eV with weak intensity. Fig. 2c shows binding energies of $Co2p_{3/2}$ and $Co2p_{1/2}$ corresponding to 778 eV and 793 eV with strong intensity. The Cu/Co atomic ratio obtained by XPS is very small and XPS results indicate that the Co_3O_4 product controlled by Cu^{2+} is relatively pure Co_3O_4.

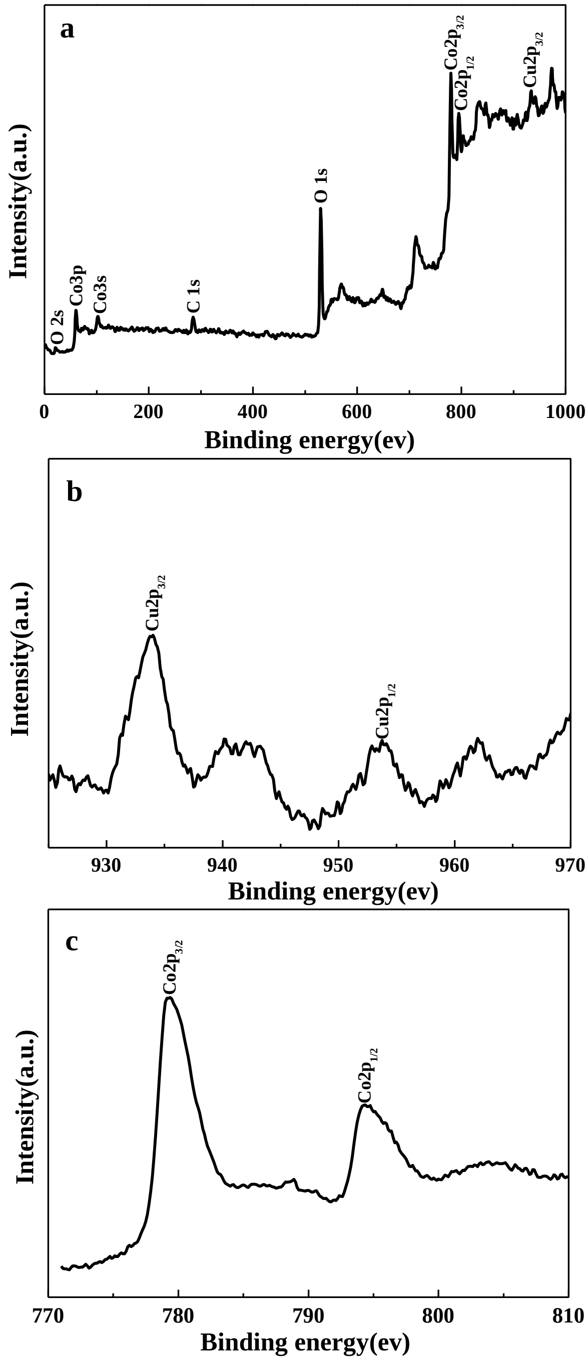

Fig. 2 (a) XPS spectrum; (b) Cu 2p spectrum; (c) Co 2p spectrum of the obtained sample.

Fig. 3a shows a representative large area SEM image of the obtained Co_3O_4, displaying that the majority of the sample is monodispersive spherical nanocrystals with an average diameter of about 400 nm. From the high-magnification SEM images shown in Fig. 3b and c, it can be seen that these nanospheres are composed of nanosheets with several nanometers in thickness.

Fig. 3d-f shows the sample's TEM images and HRTEM image, verifying that the obtained sample is monodispersive, spherical and porous. Fig. 3f also confirms that these nanospheres are composed of nanosheets with several nanometers in thickness. The HRTEM image shown in Fig. 3f inset displays one group of facet with crystal plane spacing of about 2.43 Å, corresponding to (311) facet of the cubic phase of Co_3O_4.

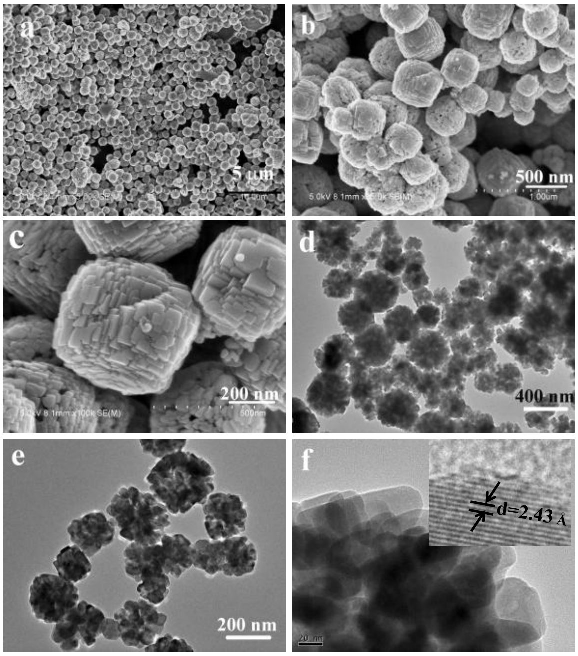

Fig. 3 (a-c) SEM images; (d-f) TEM images (inset f: HRTEM image) of the porous Co_3O_4 nanospheres.

The addition of $CuAc_2$ in the reaction system is undoubtedly the major reason for the formation of Co_3O_4 nanospheres. Without the addition of $CuAc_2$, when hydrothermally treated the mixture of $CoSO_4$ and ammonium solution, as shown in Fig. 4, only Co_3O_4 microflowers with much larger size (5 µm) and irregular Co_3O_4 nanoparticles can be obtained. With the addition of Cu^{2+}, it tends to form $CuCo_2O_4$ under alkali conditions. However, Cu^{2+} can react easily with $NH_3 \cdot H_2O$ to form $[Cu(NH_3)_4]^{2+}$ complex and resolve into the solution, so under the synthetic conditions with $NH_3 \cdot H_2O$, we can only get Co_3O_4 product. In the reaction system, metal ions would undertake the structure and surface director. It would be adsorbed to Co_3O_4 surface and induce Co_3O_4 nanoparticles to grow into nanocrystals. In order to prove our assumption that metal ions are the structure and surface-director rather than Ac^-, $CuCl_2$ and $CuSO_4$ were respectively replaced $CuAc_2$ as the additives. As shown in Fig. 5, all the obtained products are Co_3O_4 nanocrystals with spherical morphology, confirming that the existence of Cu^{2+} is the main reason for the growth of Co_3O_4 nanocrystals.

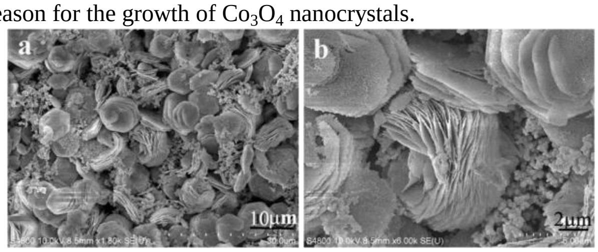

Fig. 4 (a,b) SEM images of the sample synthesized without Cu^{2+} ions.

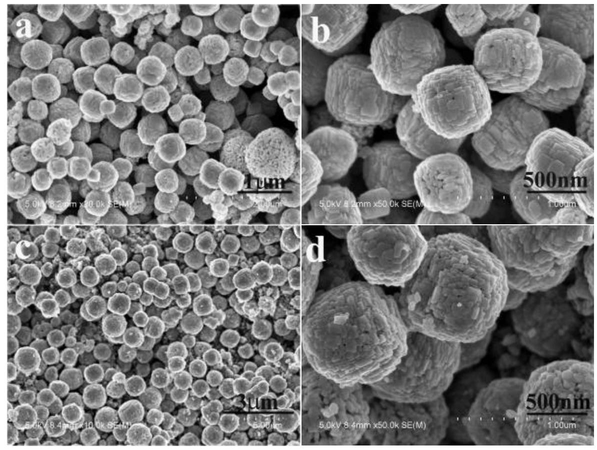

Fig. 5 SEM images of porous Co_3O_4 nanospheres prepared with different Cu^{2+} ions sources: (a, b) $CuCl_2$ and (c, d) $CuSO_4$.

In order to further certify that Cu^{2+} is the main reason for the growth of Co_3O_4 nanocrystals, we added metal salts of $CoSO_4$ to the mixture of $CuAc_2$ and ammonium solution and treated under hydrothermal conditions. The results are shown in Fig. 6. Fig. 6a~c show the SEM images of the obtained product, displaying that the majority of the sample is also monodisperse spherical nanocrystal with an average diameter of about 400 nm, which is almost the same as the typical sample with the different reaction order. Fig. 6d gives the XRD pattern of the product and all the diffraction peaks can be indexed to the cubic phase of Co_3O_4 (JCPDS 73-1701), indicating that Co_3O_4 products also can obtained under these conditions.

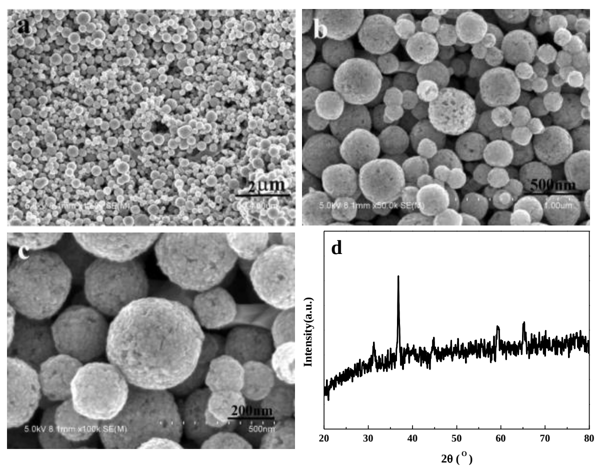

Fig. 6 (a-c) SEM images and (d) XRD pattern of the product prepared by adding $CoSO_4$ into $CuAc_2$ solution.

As known, the properties of nanostructures depend greatly on morphology and surface environments. Co_3O_4 has been extensively researched as the electrode material for lithium-ion batteries and supercapacitors.[7-11] In this paper, we studied the electrochemical properties of obtained Co_3O_4 nanospheres by applying it as the active material for supercapacitor electrode. The measurements were conducted using cyclic voltammetry (CV) in 1 M KOH electrolyte with the voltage window in 0-0.5 V and a scanning rate of 2-50 mV s^{-1}. The obtained CV curves are shown in Fig. 7. The CV curves are nearly symmetrical and display two pairs of redox peaks. The broad redox reaction peaks which come from the redox processes of Co_3O_4/CoOOH/CoO_2, are characters of the electrochemical pseudocapacitors from reversible faradaic redox reactions occurring within the electro-active materials.[20] As shown in Fig. 7a, when changing the scanning rate from 2-50 mV s^{-1}, the shape of CV curves almost do not change, maybe because the electrode material is nanosized and in favor of the electron transfer and lessens the electrode polarization. Fig. 7b shows the CV curves of Co_3O_4 nanospheres and commercial Co_3O_4 at a scanning rate of 5 mV s^{-1}. The area under the CV curve for Co_3O_4 nanospheres is apparently much larger than that of commercial Co_3O_4, which indicates that Co_3O_4 nanospheres have a higher specific capacitance than commercial Co_3O_4. This is reasonable since the unique and nano structure of Co_3O_4 could provide fast ion and electron transfer and large reaction surface area, benefiting for the electrochemical performances.

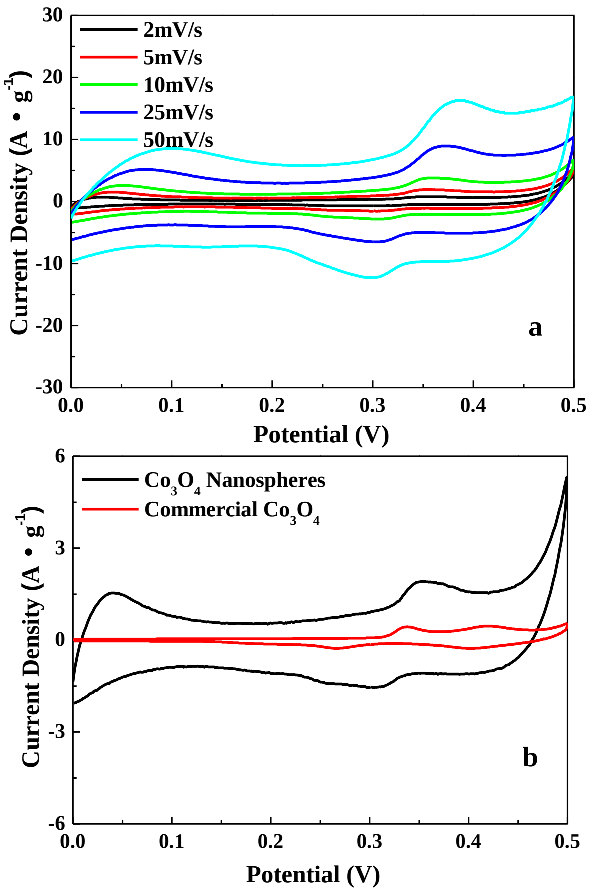

Fig. 7 (a) CV curves of porous Co_3O_4 nanospheres at scanning rate from 2-50 mV s^{-1}; (b) CV curves of Co_3O_4 nanospheres and commercial Co_3O_4 at a scanning rate of 5 mV s^{-1}.

Chronopotentiometry measurements confirm the suggestions. Fig. 8a shows charge-discharging curves of Co_3O_4 nanospheres and commercial Co_3O_4 powders obtained in potential range of 0-0.45 V in 1 M KOH at a charging-discharging current of 0.5 A g^{-1}. The shapes of the charge-discharge curves show the characteristics of pseudo-capacitance, which are consistent with the result of the CV curves. Both samples present two variation ranges during the charge and discharge steps. The sloped curve in 0-0.45 V is characteristic of typical pseudocapacitance, originating from electrochemical adsorption-desorption or a redox reaction on the electrode/electrolyte interface.[20] From the sloped curve at the discharge current of 0.5 A g^{-1}, the specific capacitances of Co_3O_4 nanospheres and commercial Co_3O_4 powders are calculated to be 246.7 F g^{-1} and 77 F g^{-1}, respectively. The specific capacitance of Co_3O_4 nanospheres is much larger than that of commercial Co_3O_4 powders, confirming the suggestion rising from the CV curves. When the discharge current density is 0.5, 1, 2, 5, 10 and 25 A g^{-1}, the specific capacitance values of the Co_3O_4 nanospheres can be calculated from the discharge curves in Fig. 8b to be 246.7 F g^{-1}, 213.3 F g^{-1}, 199 F g^{-1}, 174.4 F g^{-1}, 151.1 F g^{-1} and 105.6 F g^{-1}, respectively.

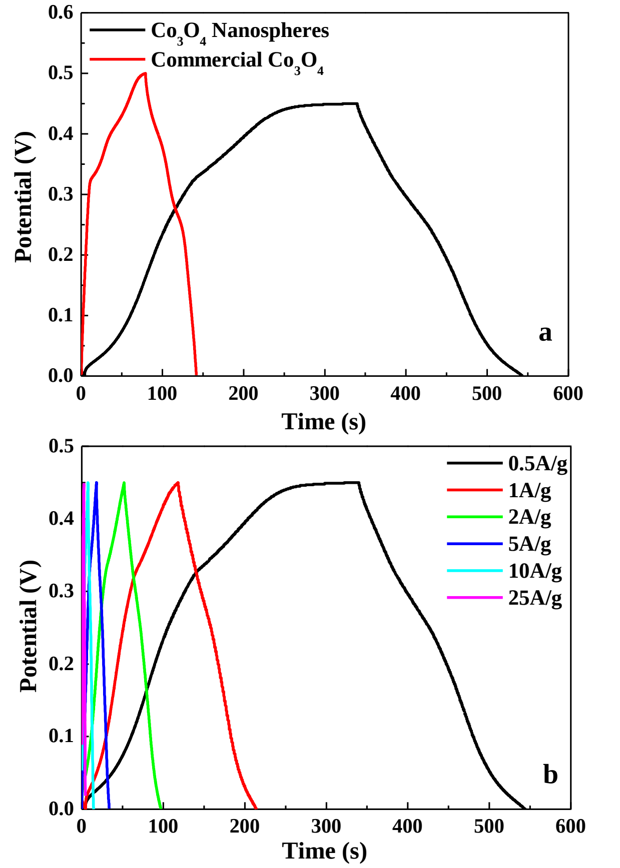

Fig. 8 Charge-discharging curves of (a) porous Co_3O_4 nanospheres and commercial Co_3O_4 powders at a charging-discharging current density of 0.5 A g^{-1}; (b) porous Co_3O_4 nanospheres at different current densities.

For the long cycle life is a very important factor of supercapacitors, the cycle charge/discharge test has also been employed to examine the service life of the Co_3O_4 nanospheres. Fig. 9 gives the variation of specific capacitance with cycle number at 1 A g^{-1} and reveals that the Co_3O_4 nanospheres electrode has good cycle properties as an excellent electrode material for electrochemical capacitors and the specific capacitance even grow a little larger in the first 500 cycles, which might be due to an electrochemical activation phenomenon.[27, 28] Clearly, Co_3O_4 nanospheres electrode holds better electrochemical capacitance performances than the commercial Co_3O_4 electrode. The high porosity structure of Co_3O_4

nanospheres minimizes both the ionic and electronic transportation distances in the cobalt oxide and thus improves the electrode kinetic performances, which is a crucial concern for high-power supercapacitor applications.

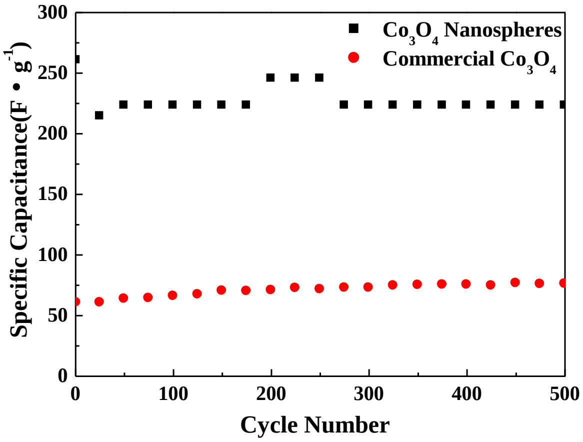

Fig. 9 Cycling properties of porous Co_3O_4 nanospheres and commercial Co_3O_4 powders at current density of 1 A g^{-1}.

Conclusions

In summary, we successfully synthesized porous Co_3O_4 nanospheres by applying metal ions Cu^{2+} as structure-inducing agents. The porous Co_3O_4 nanospheres were composed of nanosheets. In the electrochemical measurement in three electrode system, the porous Co_3O_4 nanospheres exhibit much better capacitive properties of 246.7 F g^{-1} than commercial Co_3O_4 powder at current density of 0.5 A g^{-1}, maintaining 86% of the initial capacity at current density of 1 A g^{-1} after 500 cycles. Such high performances can be attributed to the desirable morphologies. The results manifest that porous Co_3O_4 nanospheres composed with nanosheets are promising electrode material for supercapacitor in future application.

Acknowledgment

This work was supported by the National Natural Science Foundation of China (No. 21301002, 51302001 and 21441008), Anhui Province College Excellent Young Talents Fund (No. 2013SQRL037ZD and 2013SQRL036ZD) and Excellent Young Talents Support Plan of Anhui Province College.

Notes and references

1 M. Ando, T. Kobayashi, S. Iijima and M. Haruta, *J. Mater. Chem.*, 1997, **7**, 1779-1783.

2 A. M. Cao, J. S. Hu, H. P. Liang, W. G. Song, L. J. Wan, X. L. He, X. G. Gao and S. H. Xia, *J. Phys. Chem. B*, 2006, **110**, 15858-15863.

3 W. Y. Li, L. N. Xu and J. Chen, *Adv. Funct. Mater.*, 2005, **15**, 851-857.

4 S. Liu, Z. Y. Wang, H. R. Zhao, T. Fei and T. Zhang, *Sens. Actuat. B*, 2014, **197**, 342-349.

5 M. M. Natile and A. Glisenti, *Chem. Mater.*, 2002, **14**, 3090-3099.

6 L. H. Hu, Q. Peng and Y. D. Li, *J. Am. Chem. Soc.*, 2008, **130**, 16136–16137.

7 A. Q. Pan, Y. P. Wang, W. Xu, Z. W. Nie, S. Q. Liang, Z. M. Nie, C. M. Wang, G. Z. Cao and J. G. Zhang, *J. Power Sources*, 2014, **255,** 125-129.

8 X. W. Lou, D. Deng, J. Y. Lee, J. Feng and L. A. Areher, *Adv. Mater.*, 2008, **20**, 258-262.

9 H. T. Wang, L. Zhang, X. H. Tan, C. M. B. Holt, B. Zahiri, B. C. Olsen and D. Mitlin, *J. Phys. Chem. C*, 2011, **115**, 17599–17605.

10 Q. Yang, Z. Lu, X. Sun and J. Liu, *Sci. Rep.*, 2013, **3**, 3537.

11 W. Liu, L. Xu, D. Jiang, J. Qian, Q. Liu, X.W. Yang and K. Wang, *CrystEngComm*, 2014, **16**, 2395-2403.

12 A. S. Poyraz, W. A. Hines, C. H. Kuo, N. Li, D. M. Perry and S. L. Suib, *J. Appl. Phys.*, 2014, **115**, 114309.

13 J. P. Liu, J. Jiang, C.W. Cheng, H. X. Li, J. X. Zhang, H. Gong and H. J. Fan, *Adv. Mater.*, 2011, **23**, 2076-2081.

14 X. B. Zhao, Z. W. Pang, M. Z. Wu, X. S. Liu, H. Zhang, Y. Q. Ma, Z. Q. Sun, L. D. Zhang and X. S. Chen, *Mater. Res. Bull.*, 2013, **48**, 92-95.

15 R. Xu and H. C. Zeng, *J. Phys. Chem. B*, 2003, **107**, 12643-12649.

16 X. Y. Shi, S. B. Han, R. J. Sanedrin, C. Galvez, D. G. Ho, B. Hernandez, F. M. Zhou and M. Selke, *Nano Lett.*, 2002, **2**, 289-293.

17 S. Y. Xia, M. Q. Yu, J. Y. Hu, J. J. Feng, J. R. Chen, M. H. Shi and X. X. Weng, *Electrochem. Comm.*, 2014, **40**, 67-70.

18 H. S. Jadhav, A. K. Rai, J. Y. Lee, J. Kim and C. J. Park, *Electrochim. Acta*, 2014, **146**, 270-277.

19 Y. H. Xiao, S. J. Liu, F. Li, A. Q. Zhang, J. H. Zhao, S. M. Fang and D. Z. Jia, *Adv. Funct. Mater.*, 2012, **22**, 4052-4059.

20 W. Du, R. M. Liu, Y. W. Jiang, Q. Y. Lu, Y. Z. Fan and F. Gao, *J. Power Sources*, 2013, **227**, 101-105.

21 Y. Z. Zhang, Y. Wang, Y. L. Xie, T. Cheng, W. Y. Lai, H. Pang and W. Huang, *Nanoscale*, 2014, **6**, 14354-14359.

22 M. Büyükyazi, C. Hegemann, T. Lehnen, W. Tyrra and S. Mathur, *Inorg. Chem.*, 2014, **53**, 10928-10936.

23 H. W. Che, A. F. Liu, J. X. Hou, J. B. Mu, Y. M. Bai, S. F. Zhao, X. L. Zhang and H. J. He, *J Mater. Sci.-Mater. Electron.*, 2014, **25**, 3209-3218.

24 R. Xu, J. W. Wang, Q. Y. Li, G. Y. Sun, E. B. Wang, S. H. Li, J. M. Gu and M. L. Ju, *J. Solid State Chem.*, 2009, **182**, 3177-3182.

25 H. Pang, S. M. Wang, G. C. Li, Y. H. Ma, J. Li, X. X. Li, L. Zhang, J. S. Zhang and H. H. Zheng, *J. Mater. Chem. A*, 2013, **1**, 5053-5060.

26 R. M. Liu, Y. W. Jiang, H. Fan, Q. Y. Lu, W. Du, F. Gao, *Chem. Eur. J.*, 2012, **18**, 8957-8963.

27 C. C. Hu, K. H. Chang, T. Y. Hsu, *J. Electrochem. Soc.*, 2008, **155**, F196-F200.

28 H. B. Wu, H. Pang and X. W. Lou, *Energy Environ. Sci.*, 2013, **6**, 3619-3626.

Colour graphic:

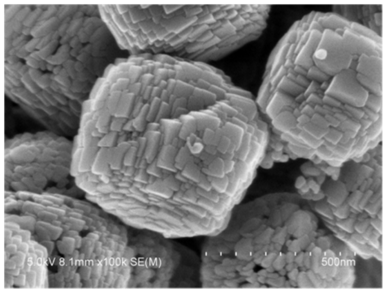

Porous Co_3O_4 nanospheres were successfully synthesized by Cu^{2+} ions as structure-inducing agents, which exhibit good capacitive properties.